

Individual Solvated Ion Properties and Specificity of Ion Adsorption Effects in Processes at Electrodes

B. E. Conway

Chemistry Department, University of Ottawa, 140 Louis Pasteur Street, Ottawa, K1N 6N5, Ontario, Canada

1 Introduction

In this article, an outline will be given on how various electrode processes, and the state and structure of electrode interphases with ionic solutions, can depend specifically on the types of ions of the electrolyte, usually anions. This specificity can be traced to the adsorption of the ions which determines (a) the structure and electric potential profile in the electrode–solution interphase and (b) the local distribution and orientation^{1,2} of solvent dipoles in this interphasial region. These effects usually influence the local concentration of ions involved as reactants in a given electrode process in the so-called ‘double-layer’ (Figure 1d) at the electrode and the activation energy of that process at a particular electrode potential.

Since an electrode reaction, cathodic or anodic, often involves, respectively, either a particular type of cation or anion, it is of much importance that knowledge of the solution and solvation properties of *individual* types of ions be known. Similarly, the structure of the electrode/solution interphase (see Figure 1), within which the electrode reaction is initiated, is determined usually in some specific way by the types of ions that populate it. The individuality of properties of ions arises principally for reasons itemized in the following paragraphs.

2 Electrode/Solution Interphase and Chemisorption of Ions

The role of individuality of ionic properties in processes at electrodes must be understood first in terms of what may be called the ‘construction’ of the electrode solution interphase, that quasi-three-dimensional region some 0.3 to 0.5 nm in thickness wherein ion adsorption and solvent molecule orientation arise (Figure 1), and where processes of ion discharge in electrolysis originate.^{3,4}

Figure 1 represents schematically how the ‘construction’ of this interphasial region can be imagined to arise from a combination of the electrode-metal/vacuum interface and the solu-

tion/vacuum (vapour) interface.³ The combination is not, however, simply ‘additive’ since contact of the electrode metal with the solution involves (a) change of the surface electron distribution at the metal interface and (b) usually complementary changes of ion and solvent distribution (and orientation) in the resulting interphase. Further, when this combination is established, the surface charge-density at the metal can be independently varied over about $\pm 0.18 e$ per atom when the electrode metal is polarized against another electrode by means of an external, controllable voltage source. The resulting distribution of ions and solvent molecules, illustrated in Figure 1d, is referred to as the ‘double-layer’⁵ (of ions and electron charges) and consists, formally, of a compact region near the electrode and a broader region (1 to 100 nm, where a diffuse, Debye–Hückel type of non-specific ion distribution arises (d, in Figure 1).

It is in the compact region (c, Figure 1 and *cf.* reference 5) that specificity of ion properties is important in determining the properties of the interphase and the kinetic aspects of Faradaic charge-transfer in electrolytic processes. The properties of ions that are of interest in this way are indicated below and are relevant to the behaviour of electrode interfaces in two ways: (I) in chemisorption of ions, usually anions, and (II) in the kinetics of discharge or formation of ions in electrolytic processes originating in the electrode/solution interphase.

In (I) the properties of importance are: (a) the charge, ze , and radius r_i of the ion, *i.e.* its charge density $ze/4\pi r_i^2$; (b) its solvation energy, *i.e.* the ion/solvent interaction energy⁶ and the related facility of deformation of its solvation coordination shell allowing the valence shell orbitals of the ion access to the electrode surface at which adsorption can then occur; (c) the so-called donicity⁷ of the ion, *i.e.* the extent to which it may undergo partial charge-transfer^{8,9} with the electrode, leading to chemisorption; and (d) the ‘hydrophobicity’^{6,8} or otherwise, of the ion, *e.g.* as with tetraalkylammonium cations, R_4N^+ .

In (II), the following properties are of significance: (a) the ionization potential or electron affinity of the species being discharged in the electrochemical reaction; (b) the overall solvation energy of the ion being discharged (or formed, depending on the direction, anodic or cathodic, of the reaction), and (c) the energy of binding of the product of the electron transfer process in (b). These factors are of major importance in determining the rate constant of the electrochemical reaction through its Gibbs energy of activation.

Of the above ionic properties, the solvation energy and the electronic properties of an individual ion are of the greatest importance in determining its adsorbability at a given electrode metal. The properties of the electrode metal are of complementary significance, in particular, the potential at which its surface bears zero charge⁵ in relation to the electrode potential at which the electrode interface is polarized *and* the electronic work function, Φ , of the metal⁴ which characterizes its electron affinity, E , in ion chemisorption processes such as equation 1 below.

3 Chemisorption of Ions with Partial Charge-Transfer

It is well known in high-vacuum surface chemistry that metal atoms such as Na^* become chemisorbed at, *e.g.*, W with virtually complete charge-transfer, at least at low coverage, so that the chemisorbed state is, *e.g.* $W(e^-)Na^+$. This state, and the asso-

Dr. Conway was born in London in 1927 and studied at Imperial College, London (Ph.D., 1949; D.Sc., 1961). In 1956 he joined the University of Ottawa (becoming Full Professor in 1962) where he is presently Alcan–NSERC Research Professor of Electrochemistry.

In 1968 he was elected Fellow of the Royal Society of Canada. He was the recipient of the Chemical Institute of Canada Medal in 1975, the American Chemical Society Kendall Award in Surface Chemistry in 1983 and the Henry Linford Medal of the Electrochemical Society in 1984. In 1989 he was awarded the Electrochemical Society's Olin Palladium Medal and, in 1991, the Italian Chemical Society's Luigi Galvani Medal. In 1969–70, he was Commonwealth Visiting Professor at the Universities of Southampton and Newcastle upon Tyne.

His principal areas of research have been in the field of interfacial electrochemistry, electrochemical surface science and electrode kinetics, and the characterization of individual solvated-ion properties in aqueous solution in relation to ionic adsorption.

He is the author of some 300 scientific papers and 3 research monographs, and is co-editor of the Modern Aspects of Electrochemistry review series.

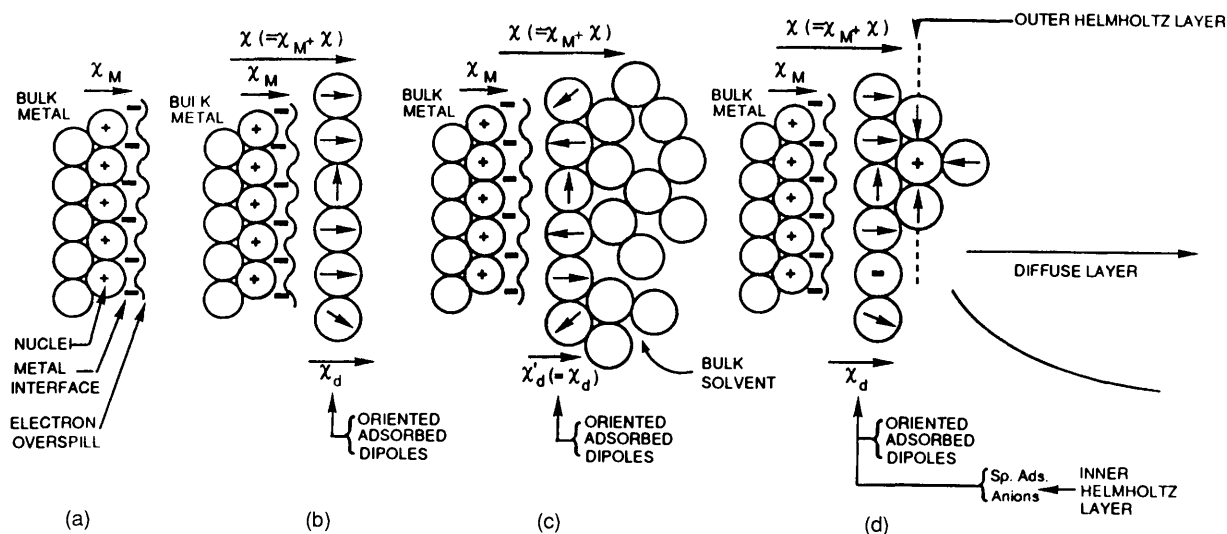


Figure 1 Construction of the electrode/solution interphase, illustrating the generation of the electrical double-layer at an electrode. (a) Metal/vacuum interface. (b) Metal/vapour interface with adsorbed water dipoles. (c) Metal surface with bulk dipolar solvent. (d) Metal/solution interphase, with adsorbed solvent (H_2O) molecules and ions, and diffuse-layer ion distribution beyond the compact layer.

ciated energy of chemisorption, is determined by the difference of work of function of W and the ionization energy of Na^+ . A corresponding coverage-dependent surface potential, χ_s , arises. At electrodes, a similar situation arises as illustrated in equation 2 below, except usually a partial extent, δ , of electron charge-transfer takes place although, for radicals with low electron affinity, e.g. I^\cdot , the corresponding ion, I^- , is chemisorbed, as found at Pt, with virtually complete charge-transfer. The range of degrees of partial charge-transfer involving anions and other species at Hg and other metals, expressed as the so-called 'electrosorption valency', γ , is represented as a function of electronegativity difference $\chi_M - \chi_s$ in Figure 2 according to Schultze and Koppitz.¹⁰

From a thermodynamic point of view, the 'electrosorption valence',¹⁰ γ , related to δ in equation 2, is defined by

$$\gamma = -\frac{1}{F} \frac{\partial q_M}{\partial \Gamma} E \equiv \frac{1}{F} \frac{\partial \mu_A}{\partial E} \Gamma \quad (1)$$

where q_M is the metal surface charge-density, E the potential, Γ the surface excess of adsorbed ion and μ_A the chemical potential

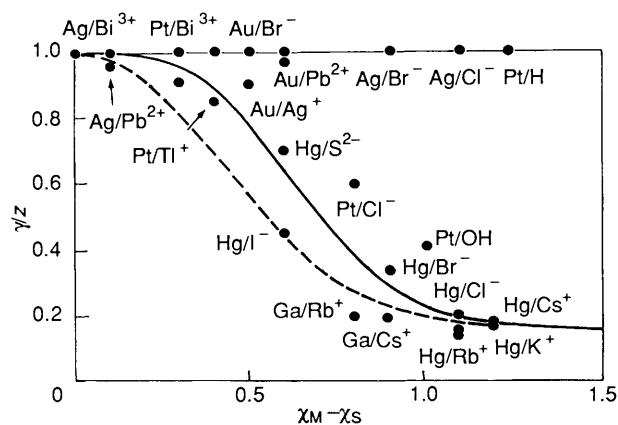


Figure 2 Electrosorption valency for ion, and H and OH, adsorption at electrodes as a function of the appropriate electronegativity difference.

(From reference 10, with added data.)

of A^- (or a salt of A^-) in solution. γ can be related¹⁰ to δ through some model of the double-layer.

The process of charge-transfer^{9,10} can be represented formally as:



where a charge $(1 - \delta)e$ has been transferred to the Fermi level of metal M leading to a change of the surface dipole moment at M [normally, at electrode metals, an intrinsic surface moment already exists, coupled with a component due to solvent-molecule orientation (see Figure 1)]. Also, the hydration of A^- will normally be diminished ($m\text{-H}_2\text{O} < n\text{-H}_2\text{O}$), depending on the magnitude of δe in relation to e .

The energy quantities driving the process shown in equation 2 are principally the electron affinity of the metal ($-\Phi$), the electron affinity, E , of the radical A^\cdot and the hydration energy of A^- ; i.e. the energy change $\Delta U(2)$ for the process is

$$\Delta U = -(1 - \delta)\Phi_M + (\delta - 1)E + (m - n)S + \Delta \quad (3)$$

where S is the mean hydration energy (per H_2O) of A^- and Δ is the energy of the new interaction between $\text{A}^{\delta-}$ and the electrode metal as a result of process (2). In equation 3 E and S quantities are negative and Φ positive. Δ will tend to be negative, i.e. exoenergetic.

Individual ionic effects at electrodes are commonly manifested in the following ways:

- Shift of the potential (p.z.c.) at which the electrode interface bears zero charge;^{5,11}
- Modification of the double-layer capacitance behaviour,⁵ often resulting in:
- Modification of kinetics of an electrode process,⁴ e.g. H_2 evolution or surface oxidation;
- Changes of relative reflectivity, and ellipsometric parameters,¹² viz. change of phase angle Δ and of amplitude ψ ;
- Modification of so-called underpotential deposition profiles^{3,13} of current vs. potential, e.g. for deposition of sub-monolayers of H on Pt or Pb on Au;
- Specificity of ionic properties is manifested in ion-binding in ion-exchange resins and membranes,⁶ at linear polyelectrolytes and proteins, and in macrocyclic ligand molecules such as the so-called 'crown-ethers' and 'cryptands',⁶ and also in biologically significant molecules such as valinomycin which act as ion carriers through the lipid membranes of living cells.⁶ Even such pairs of ions as Na^+ and K^+ , or Mg^{2+} and Ca^{2+} , commonly regarded as chemically very similar, are distinguished by substantially different behaviour in biological systems, e.g. for Na^+ and K^+ in active transport of ions across

the neurone membrane, or for Mg^{2+} and Ca^{2+} in ion binding, *e.g.* to myosin and other polypeptides.

One of the clearest examples of specificity of ion behaviour at electrodes arises from adsorption of anions at the Hg/H₂O interface⁵ and is manifested in the shift of the p.z.c. of Hg¹¹ illustrated in Figure 3a. An hierarchy of effects arises depending on the properties of the ion delineated in (I) above. The shifts ΔE , are measured in volts with respect to the p.z.c. of Hg in an electrolyte, *e.g.* NaF, the ions of which are insignificantly chemisorbed at Hg.⁵ The largest shifts arise with the most polarizable and donative ions, SH⁻, CNS⁻, I⁻. These ion adsorption effects also have major influences on the kinetics of electrode reactions at Hg, *e.g.* the discharge of the aqueous proton, H₃O⁺, in the cathodic H₂ evolution reaction.

The changing population of anions and cations at an electrode interface as its surface charge is varied in response to modulation of electrode potential, is manifested as a capacitance: the capacitance, C , of the double-layer (Figure 1d). Measurements of C give sensitive information⁵ on the specificity of ion adsorption effects at the electrode surface and on the structure of the electrode/solution interphase as exemplified by the capacitance plots shown in Figure 3b for several 1:1 electrolytes at Hg. Similar anion-specific behaviour is manifested in the surface-excess entropies and volumes of the interphase at Hg, especially at potentials positive to the p.z.c. where the Hg bears a positive excess charge, leading to anion chemisorption. This ion-specific information is complementary to that provided by the hierarchy that arises in p.z.c. values for various electrolytes as illustrated in Figure 3a and discussed below.

It should be mentioned that the shapes of the capacitance *vs.* potential curves of Figure 3b are determined by the following three principal factors: (i) The combination of the concentration-dependent diffuse-layer component, C_{diff} , of the overall C (corresponding to the 1-dimensional ionic atmosphere excess charge conjugate to the 'excess' (\pm) electronic charge density at the metal surface, giving rise to a minimum in C at the p.z.c.) with the compact layer component, $C_{compact}$. (The combination is a 'series' one: $1/C = 1/C_{diff} + 1/C_{compact}$.) (ii) The compact layer capacitance at potentials positive to the p.z.c., *ca.* 35 to 45 $\mu F cm^{-2}$. (iii) The compact layer capacitance at potentials negative to the p.z.c., *ca.* 18 to 30 $\mu F cm^{-2}$, depending on the electrode metal. The hump in the C *vs.* E profile, *e.g.* seen clearly in the case of NaF solutions (Figure 3b), is believed to be connected with solvent dipole reorientation and local solvent structure change, *e.g.* with NO₃⁻ or ClO₄⁻, but is strongly influenced by chemisorption of the anions. Strongly adsorbed anions, *e.g.* I⁻, CNS⁻, lower the capacitance through interaction with the surface and with co-adsorbed solvent molecules (Figure 1d) so a complex situation then arises.

Values of the compact double-layer capacitance contribution can be separated using the 'series' relationship shown above and employing a theoretically calculated⁵ value of C_{diff} which can be done quite reliably. $C_{compact}$ represents the differential coefficient $dq_{compact}/dE$, where q is the charge associated with ion accumulation in the compact layer. By use of appropriate electrochemical thermodynamic relations,⁵ the anion contribution in $q_{compact}$ can be evaluated for various electrolyte concentrations and electrode potentials, E . Values of q can be directly related to the respective surface excesses Γ ($zF\Gamma = q$) and thus to surface coverages by the adsorbed ions. The only other factor that may complicate this operation is the value of the electroadsorption valence γ involved in equation 1.

With further operations on the data, the adsorption isotherm and 2-dimensional equation of state for anions in the compact region of the interphase can be determined. It is significant to note that the capacitance, being a *differential* quantity, provides sensitive information on the form of the adsorption isotherm applying to the accumulation of anions at electrode interfaces, especially at potentials positive to the p.z.c.

Classically, one of the most significant indications of ionic chemisorption effects is that provided by the 'hierarchy' of shifts of p.z.c. of the Hg/water interface for a given concentration of

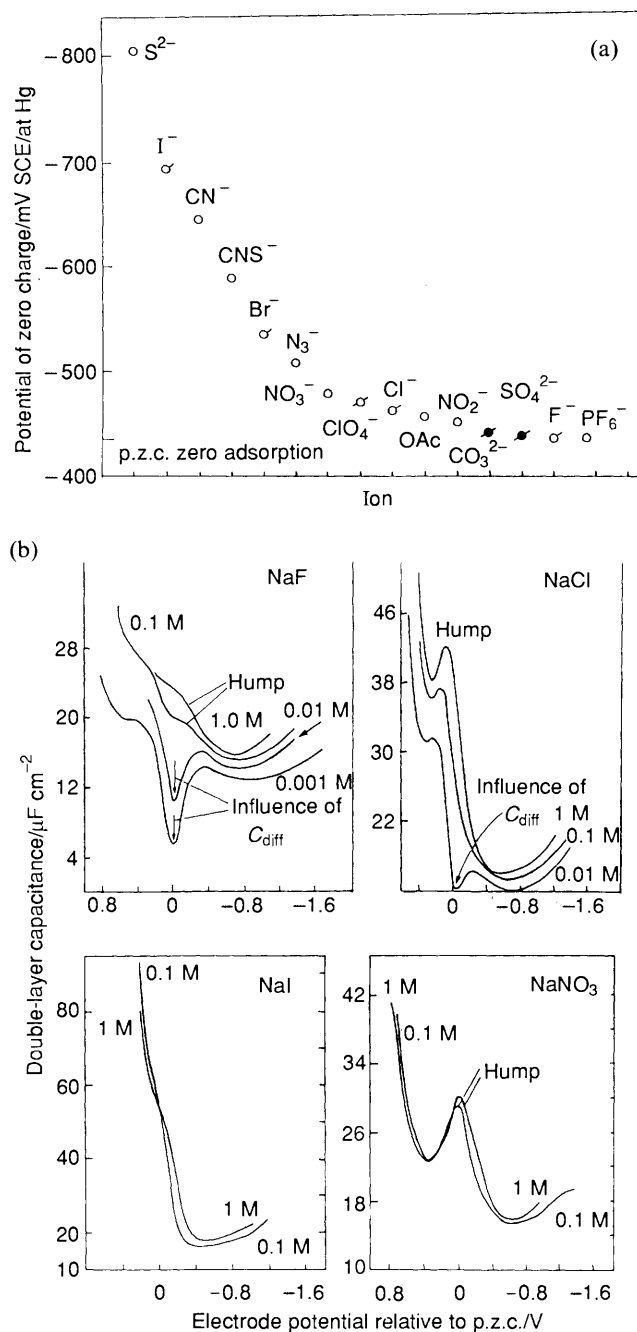


Figure 3 Examples of specificity of anion interaction with the Hg electrode surface. (a) Hierarchy of shifts potential of zero charge of Hg due to adsorption of various anions from aqueous electrolytes (based on data from reference 11). (b) Profiles of double-layer capacitance at Hg as a function of potential for aqueous NaF, NaCl, NaI, and NaNO₃ (298 K) (from Grahame, reference 5). (Minima in dilute solutions are due to the then predominant C_{diff} .)

simple salts of the indicated anions, as illustrated in Figure 3a and referred to above, for the series of anions from PF₆⁻ to S²⁻ or SH⁻. A combination of changes of hydration energy and hydrated-ion structure,⁶ electron-pair donicity,⁷ polarizability, ionic radius, and charge is involved, with changing identity of the ions. Amongst other factors, Barclay¹¹ has identified the relative 'hardness' or 'softness' of the anions (in the Basolo-Pearson terminology, related to Lewis basicity and donicity) in determining their adsorbability, characterized by their standard Gibbs energies of adsorption. The solvation energy of the ions and (especially) the *deformability* of the solvation shell as the ion interacts with a metal electrode surface, are of equal importance as these determine (a) how close the charge-bearing centre can

approach the 'electronic surface' (the electron overspill plane, Figure 1a), of the electrode metal, and (b) what is the resulting specific interaction of the electron pairs of the ion with the metal surface and any classical electrostatic image interaction.

Usually, for anions, these factors are not independent, as hydration energy depends in a complex way on ionic radius (through the ion-solvent dipole, ion-quadrupole, and longer-range Born dielectric polarization energy* components⁶) and, for anions, A^- , increasing ionic radius is also usually associated with increasing Gutmann donicity⁷ of lone-pairs, increasing polarizability, and decreasing electron affinity of the radical, A^\cdot . As ionic size increases, donor electron pairs become more accessible to the electrode due to the greater ease of deformability of the coordinating solvent-dipole co-sphere while the intrinsic Lewis-base strength tends also to increase.⁷ Hence, in ionic adsorption, there is a close but complex coupling between the electronic and solvational properties of the ion, each of which is related to ion charge density and the position of the element from which the ion originates in the Periodic Table.

Additionally, the hierarchy of adsorbability of anions at Hg, shown in Figure 3, is not necessarily the same as at other metals, e.g. Au or Pt. The specific effects depend on the work-function of the metal, the emergent orbital distribution at its surface as well as on the ionic properties referred to earlier.

As a consequence of these cross-interaction effects, it is difficult to make reliable *a priori* calculations of energies of specific adsorption of ions, although some attempt to do this was made by Anderson and Bockris,¹⁴ taking into account hydration energies and other factors, while Schmickler¹⁵ has made quantum-chemical calculations on this problem. Analogous problems arise in calculation of salt solubilities which are usually highly specific for various salt-pairs of ions.

The fact that cations, of a given charge and radius, are usually much less strongly chemisorbed than anions of comparable radii (but the range of ions for which such radii⁵ are comparable is strictly limited with simple ions) is to be attributed to (a) the stronger orientational force constants^{16,17} for solvent-dipole/ion interaction (smaller deformability) and the substantially smaller (or negative) donicities of cations (they are Lewis acids) than of anions.

4 Determination of Individual Ionic Properties in Solution

Evaluation of individual solvated ion properties is required for interpretation of a number of aspects of electrode processes and electrosorption. For determination of so-called thermodynamic properties of ions in solution, a quite general fundamental problem is involved⁶ in that any experiments that can be devised give the mean or geometric mean of the values for the cations and anions of the electrolyte. This arises because the thermodynamic properties of an electrolyte are determined by the chemical potential, μ , and the standard value, μ° , of both the cations and the anions of the electrolyte together and, in a coupled way, by the chemical potential of the solvent as in measurements of vapour pressures or freezing points of salt solutions. That is,

$$\mu_{\text{salt}} = \mu_{\text{salt}}^\circ + RT \ln a_{\text{salt}} \equiv \nu_+ \mu_{\text{c}}^\circ + \nu_- RT \ln a_+ + \nu_- \mu_{\text{a}}^\circ + \nu_- RT \ln a_- \quad (4)$$

for a salt of stoichiometry $M^{z+}_\nu A^{z-}_\nu$, fully dissociated in solution. Experimentally, only μ_{salt} or μ_{salt}° , or their derivatives with respect to temperature (giving the partial molal entropy and enthalpy) or to pressure (giving the partial molal volume), are accessible experimentally, e.g. by means of EMF measurements employing the Nernst equation or, less directly, by means

of freezing point or vapour pressure experiments, employing the Gibbs-Duhem equation which relates changes of μ of the solvent to changes of μ of the solute with changing composition.

Although electrodes reversible to one kind of ion are available for electrochemical thermodynamic EMF measurements and sense the chemical potential of that ion, the above general thermodynamic problem cannot be avoided since EMF determinations always require the difference of potential between two dissimilar electrodes.

However, complementary to the thermodynamic properties of ions in solution, are the hydrodynamic transport (e.g. ionic mobilities and transference numbers in conductance measurements, diffusion constants) and spectroscopic properties (e.g. infrared and Raman spectral behaviour⁶ and nuclear magnetic resonance behaviour,⁶ such as chemical shifts¹⁸ and nuclear magnetic relaxation times) together with the dielectric behaviour of ions in solution (change of dielectric constant of the solvent or dielectric rotational relaxation times of the solvent molecules⁶ in the presence of ions).

The above properties are not subject to the fundamental limitation inherent in estimation of ionic thermodynamic properties but difficulties still arise in interpreting e.g. solvent optical⁶ and NMR¹⁸ spectral changes, and solvent dielectric properties since these are usually influenced by both types of ions of the electrolyte in not directly separable ways. However, by means of experiments on a series of salts having either a common cation (NaF, NaCl, NaBr, NaI) or a common anion (LiCl, NaCl, KCl, RbCl, CsCl, $\text{Me}_4\text{NCl} \dots \text{R}_4\text{NCl}$), useful individual ionic trends in such properties can be quantitatively identified.^{6,19} However, by examination of the NMR behaviour of a suitable isotope of the individual type of ion itself, e.g. ^{23}Na , ^{31}P (in phosphate), much less ambiguous information can be obtained, but of a different but complementary kind.

Basically, in the spectroscopic and dielectric methods, the aim is to evaluate the specific aspects of ion-solvent (usually H_2O or CH_3OH) interaction such as: (i) time-average coordination of the ion by solvent molecules; (ii) mean orientation of solvent molecules in the ion's first coordination shell;¹⁷ (iii) possible partial electron-transfer^{9,10} between the ion and the solvent (related to the Lewis 'donor-acceptor' behaviour of the ion and its coordinated solvent molecules, especially in transition-metal cation solvation); (iv) general electrostatic polarization of the solvent, e.g. giving rise to ^1H or ^{17}O chemical shifts in NMR experiments,¹⁸ or to vibrational and librational frequency shifts in optical spectral behaviour; and (v) local modifications of solvent structure near the ion. The NMR effects arise principally from electronic polarization associated with the interaction between the ion and the solvent, causing a change in local magnetic field at the resonant nucleus due to electronic shielding, an effect that is manifested as a 'chemical shift' in the resonant frequency or in the corresponding magnetic field required for magnetic resonance at a particular instrumental frequency.

A major direction of research on individual ionic properties in solution has involved attempts to introduce some extra-thermodynamic principle, having some relatively sound theoretical basis, by which some thermodynamic property for the salt can be separated into its ionic component values. Procedures of the above kind were critically reviewed¹⁹ by the present author, with estimates of their reliability.

An early suggestion for evaluation of individual ionic properties was to split salt values equally, e.g. for a salt such as KF that has almost equal radii of its two ions. However, this procedure is quite unsatisfactory as it is now known that the hydration energy of F^- is substantially larger (more negative) than that of K^+ due to the non-cancellation of ion/ H_2O -quadrupole interactions in reversal of charge from K^+ to F^- . Even splitting of the salt value for $\phi_+ \text{A}^+ \cdot \phi_- \text{B}^-$ has been questioned on the basis that the interactions of the cation and anion with water are not identical as indicated e.g. by NMR experiments. More sophisticated methods are therefore required and they depend on what property is being evaluated.

* According to Born's theory, ionic solvation energy arises on account of loss of the electrostatic 'self-energy' of the ion upon introduction of the ion into a solvent dielectric medium. The effect is due to the electrostatic polarization induced in the medium by the ion's field, corresponding to electronic and dipole orientation polarization of the solvent molecules.

Various extrapolation procedures have been employed, based on proportionality of the value of the property to some function of ion size or radius, e.g. for individual ionic volumes or less satisfactorily (based on the Born dielectric polarization equation⁶) for partial ionic Gibbs energies of ions in solution. Partial ionic entropies are the least subject to error as they can be obtained with little uncertainty from the EMF values of non-isothermal cells, especially when a saturated salt-bridge thermal junction is employed. The latter procedure is based on measurement of the EMF of a cell comprising two identical reversible electrodes, e.g. H_2 , H^+/Pt , but at different temperatures. The temperature coefficient $F.dE/dT$ is then related to the entropy change in the half cell reaction $\text{H}^+_{\text{aq}} + e \rightleftharpoons \frac{1}{2}\text{H}_2$, for which the partial molal entropy \bar{S}_{H^+} (or its standard value, $\bar{S}^{\circ}_{\text{H}^+}$) can be quite reliably evaluated.¹⁹ Since \bar{S}° for a salt, or acid, pair of ions can be unambiguously evaluated, knowledge of one individual ionic value, e.g. \bar{S}_{H^+} , enables, in principle, all other ionic values to be determined. Data for non-aqueous media are, however, scarce.

Unfortunately, quantities such as ΔG° and ΔH° for individual ionic solvation, that are required for interpretation of energies of activation of ion-discharge processes or energies of adsorption, are the least well founded,¹⁹ with uncertainties of at least $\pm 20 \text{ kJ mol}^{-1}$ or 0.22 V for a one-electron process. Values of these functions are of major importance in interpretations of energies and entropies of activation in Faradaic electrode processes which involve solvational reorganization or elimination of solvation as in proton discharge in water electrolysis.

Interpretation of activation energies, especially for proton transfer, requires not only the overall individual energy of ionic solvation but its variation with the normal coordinates of the ion-solvate complex, or for H^+ , with the position of the proton being transferred along the reaction coordinate, coupled with relaxation of associated H_2O molecules, a process complicated by the possible involvement of quantum-mechanical tunnelling of the proton. Treatments for electron transfer at outer-sphere complex ions are in some ways simpler and have been based, in earlier work, on the Born energy of solvation; this is now believed to be a serious oversimplification as 'reorganization processes' involving the ligands themselves, including H_2O in aquo-complexes, must be significantly involved as indicated from volume of activation studies.²⁰

It will be useful to give several examples of evaluations of individual ionic properties. In the case of ionic volumes, the most reliable method^{19,21} has been that in which the infinite-dilution partial molal volumes of a series of symmetrical, homologous tetraalkylammonium halides (X^-), $\text{R}_4\text{N}^+\text{X}^-$, are plotted against either the molecular weight of the cation or the number of C atoms in the 4 R groups (Figure 4), to zero; the intercept on the volume axis is then the partial molal volume of the co-anion, X^- . With such a value, $V^{\circ}_{\text{X}^-}$, and any other values for suitable salts M^+X^- , values for any other ions in non-associated electrolytes can be obtained by additivity principles. A complementary method employs measurements of the so-called 'ionic vibration potentials', $\Delta\phi_i$, in solution, generated by subjecting an electrolytic solution to a beam of ultrasonic radiation.²² $\Delta\phi_i$, coupled with salt solution density measurements, gives the difference and sum of solvated ion volumes, from which individual ionic volume data can easily be calculated.^{6,12} From values of ionic volumes in solution and knowledge of individual crystal ionic volumes (the intrinsic volumes of ions), it is possible to derive ion solvation-shell volumes and the so-called electrostriction⁶ that the ion causes in the solvent, i.e. the molal volume decrease, ΔV°_e , of the solvent, per gram ion, due to the electrostatic polarization tension that arises when the ion is introduced into the solvent at infinite dilution.

Figures 5a and 5b show plots of two individual ionic properties as a function of ionic radius as examples, while Figure 6 shows how the ^1H NMR chemical shift of water depends on the volume of R_4N^+ cations at various temperatures. It is usually found, as exemplified here, that the dependence of the given property on ionic radius is different for a series of univalent

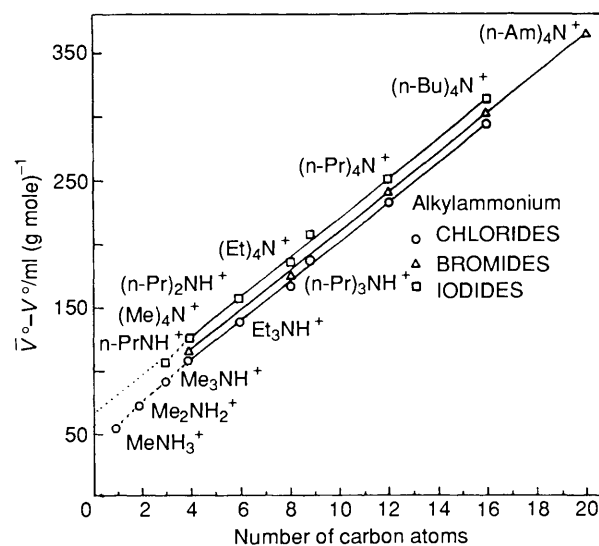


Figure 4 Extrapolation of infinite-dilution partial molal volumes of a series of homologous, symmetrical tetraalkylammonium bromides to zero number of C atoms in the R groups.²⁶ (From reference 26.)

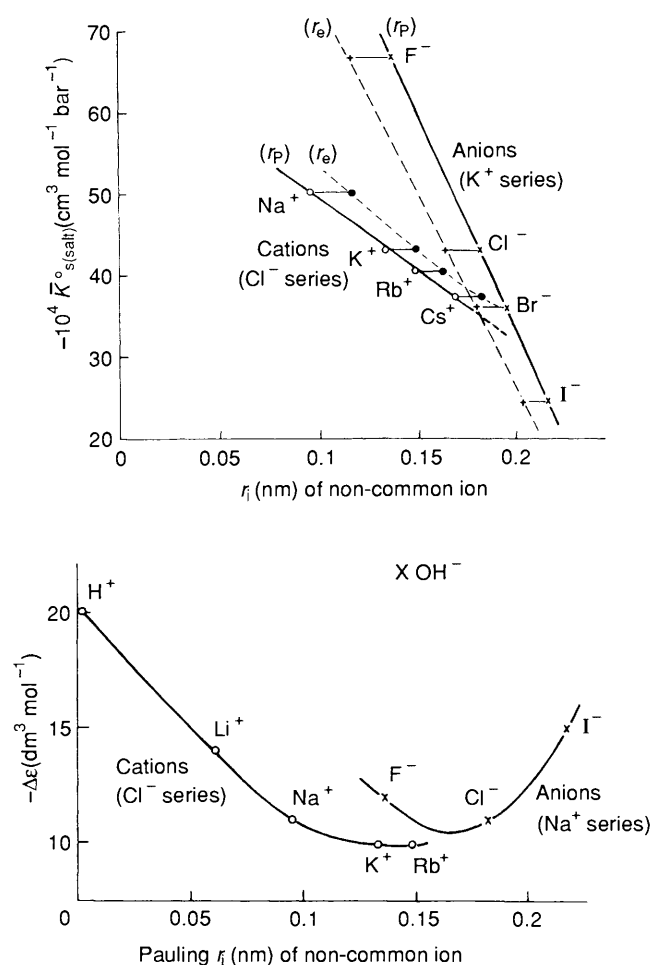


Figure 5 (Top) Plot of partial molar isentropic compressibility, $\bar{K}^{\circ}_{s,\infty}$ at ∞ dilution for alkali halides as a function of ionic radius of the non-common ion (r_p = Pauling ionic radii; r_e = electron-density ionic radii). (Bottom) Plot of change of dielectric constant $\Delta\epsilon$ at 1 mol dm^{-2} concentration of cations and anions in water at 298 K . (From references 6 and 19.)

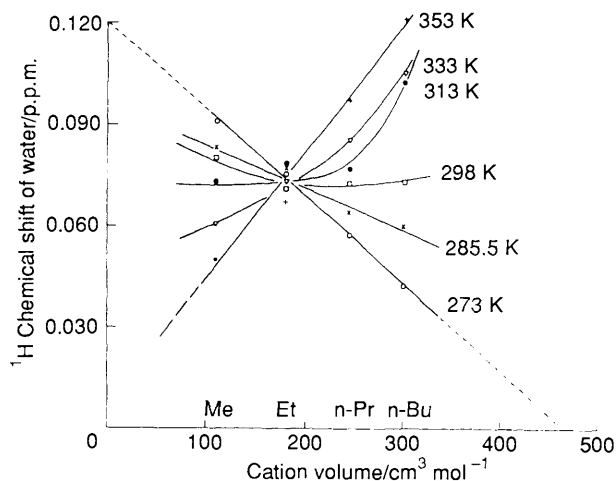


Figure 6 Plot of ^1H chemical shift of water at various temperatures for a series of symmetrical R_4N^+ bromides as a function of cation volume. Internal reference; CH_3 protons on R groups. Extrapolations of data for 273K give hypothetical chemical shift for zero cation size or hypothetical ion size for zero shift.

(From J. Davies, R. Ormondroyd, and M. C. R. Symons, *J. Chem. Soc., Faraday Trans. 2*, 1972, 68, 686.

cations from that for a series of corresponding anions. This behaviour arises on account of the substantially different effects that cations and anions of similar size and the same but opposite charge have on the orientation of water dipoles and resulting local breaking or bending of H-bonds. This type of difference is important in considering the structure of electrode/solution interphases on the positive (with anion adsorption) relative to the negative (with cation adsorption) side of the p.z.c. as the electrode potential is varied.

5 Solvational Specificity in Ion Adsorption

Earlier, reference was made to the role played by the facility with which deformation of the solvation shell of the ion takes place, in determining the order of strengths of ion chemisorption. The specificity of the solvational aspect of the properties of the ion is interestingly demonstrated by the order of adsorption behaviour of ions at the air/water interface as manifested in the measurable changes, Δ , of surface potential, χ_s , of the air/water interface²³ and the values of air/water interfacial tensions.

The value of $\Delta\chi_s$ for salt ion adsorption at air/water interfaces is determined (a) by an ionic double-layer²⁴ set up near the surface of the water, corresponding to charge-separation between the solvated cations and anions across (but within) that interphase (due to their different affinities for the solvent and different radii), and (b) by different specific electrostatic modifications of the intrinsic solvent dipole orientation in the interface of the solvent liquid, itself, brought about by the surface excesses of the cations and anions. The electrostatic factors involved, including electrostatic image interactions, have been discussed by Wagner and by Onsager and Samaras,²⁵ Conway,²⁶ and Bell and Rancecroft.²⁴

In Figure 7 this matter is illustrated by the results of Jarvis and Schieman²³ for $\Delta\chi_s$ for a number of salts, some as a series with common anions or with common cations. It is clear that $\Delta\chi_s$ for the air/water interface already depends very much on the type, radii, and solvational properties of the ions in water, *i.e.*, in the absence of any specific interactions with a metal-electrode 'wall'. Hence the specificity of anion adsorption at Hg and other metals must be attributed significantly to the specificity of the *ion-solvent* interaction and structure of the ion-solvent co-sphere, as well as from the electronic and electrostatic (image or equivalent) interactions that arise at the metal. In the latter case, a complicating factor is, of course, that the metal itself has orientationally specific interactions with solvents such as water,

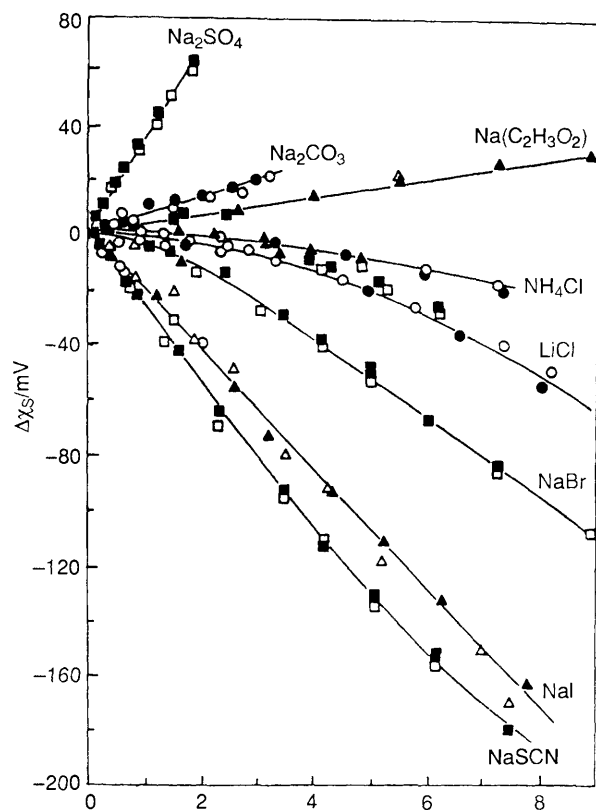


Figure 7 Surface potential changes, $\Delta\chi_s$, for salt ion adsorption at the air/water interface as a function of concentration. (Redrawn from reference 23.)

as shown by Trasatti.² This solvent-dipole orientation, together with its associated local librational entropy,¹⁶ depends also on q_M at the metal and can be ion dependent²⁶ on account of ion-specific solvation co-sphere interactions.

An important class of specific interactions of ions with electrode metal and other surfaces arises with so-called 'hydrophobic' ions.⁸ These are ions that have an hydrophobic coordination region around the charge as in the case of tetraalkylammonium cations (R_4N^+) or tetraphenylborate or arsonium ions, $\phi_4\text{B}^-$, $\phi_4\text{As}^+$. Such ions tend to 'escape' from aqueous media in which they are dissolved as salts either to the air/water interface or, if an electrode is present, to become adsorbed in the double-layer where they can minimize their unfavourable interactions with the H-bonded network of water molecules of the solvent. The effect is analogous to micelle formation with *e.g.* long-chain alkyl carboxylates, which arises from minimization of unfavourable alkyl-group/ H_2O -structure interactions and maximization of van der Waals interaction between the alkyl chains.

6 Electrostriction of Ions in Solution and in the Double-Layer

The individuality of solvation behaviour of ions is manifested, amongst other ways, but especially significantly, in the volumes (and entropies) of ions in solution which usually differ from their respective crystal ionic volumes on account of the electrostriction of solvent, giving rise to the volume decrease, ΔV_e , referred to earlier. Usually, the ΔV_e for ions is closely related to their respective entropies of solvation due to a self-compression effect (see below).

The electrostriction effect arises, formally, on account of an electrostrictive pressure (tension), P_E , associated with a field E in a dielectric being given by $P_E = E^2(\epsilon - 1)/8\pi$ where ϵ is also usually a $f(E)$.⁶ Near ions, E can be up to $ca. 3 \times 10^7 \text{ V cm}^{-1}$. Mechanistically, it arises from the tendency of solvent dipoles to be concentrated in the high field region of a field gradient; also

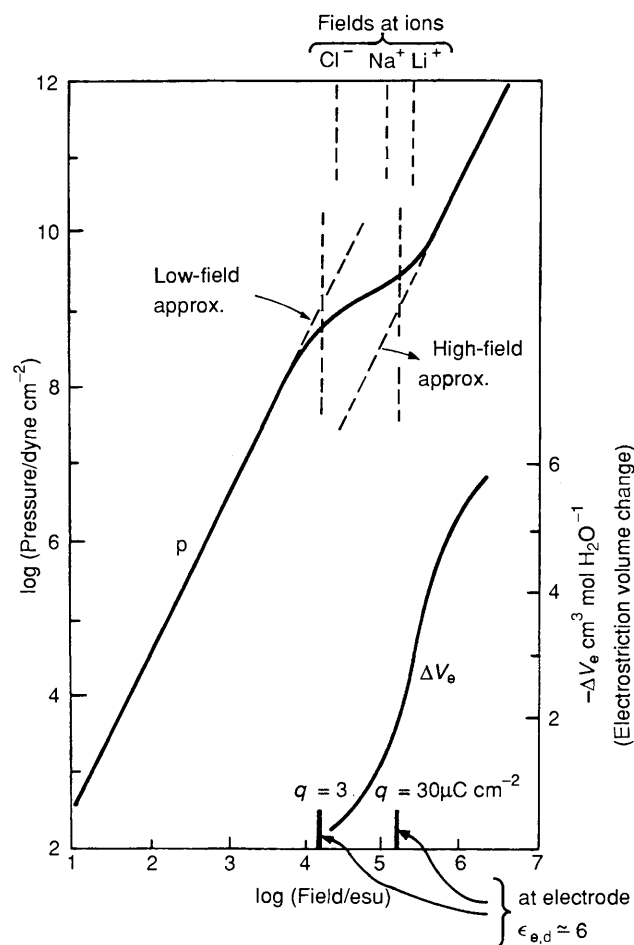


Figure 8 Electrostrictive pressure, P_E , and electrostriction volume, ΔV_e , as a function of field E at ions and at an electrode surface for various q_M values. (Calculated on the basis of the treatment given in reference 27.)

dipole orientation at ions, in water, leads to structural volume changes in the H-bonded water lattice. Similar effects arise in the double-layer interphase (Figure 1d) at electrodes.

It is of interest to compare the electrostriction at ions with that of solvent in the double-layer at electrodes, due to the field and field-gradient of the electrode. The importance of electrostriction in the double-layer, coupled with diminution of dielectric constant at high fields, was the basis of Macdonald's simulation of the usually observed (*cf.* reference 5) hump in the dependence of compact-layer capacitance of the double-layer at Hg on electrode potential. Electrostriction volumes, ΔV_e° , at ions can be evaluated as indicated earlier but the required \bar{V}_i° data must be derived from experimentally determined \bar{V}_i° data for an appropriate salt, using a procedure^{19,21,22} for separating the infinite-dilution anion and cation \bar{V}_i° values, as described earlier.

The electrostatic pressure, P_E , due to a field, E , in a polar dielectric medium can also be evaluated, taking account of the pressure and field dependence of the dielectric permittivity.²⁷ This leads to an *a priori* basis for evaluation of ΔV_e° ; P_E and ΔV_e° , both as a function of E , as shown in Figure 8. The inflection in the P_E vs. E curve at high E values arises when the orientation polarization energy exceeds the average thermal energy kT .

Also shown are estimates of the fields in the primary hydration cospheres of Li^+ , Na^+ , and Cl^- (top scale) and the range of fields in the compact layer region of an electrode interphase bearing surface charge-densities, q_M between 3 and $30 \mu\text{C cm}^{-2}$ (lower scale). Electrostriction in the electrode interphase is evidently comparable with that at small ions in the range of q_M accessible⁵ at Hg. Unfortunately, it is not possible experimen-

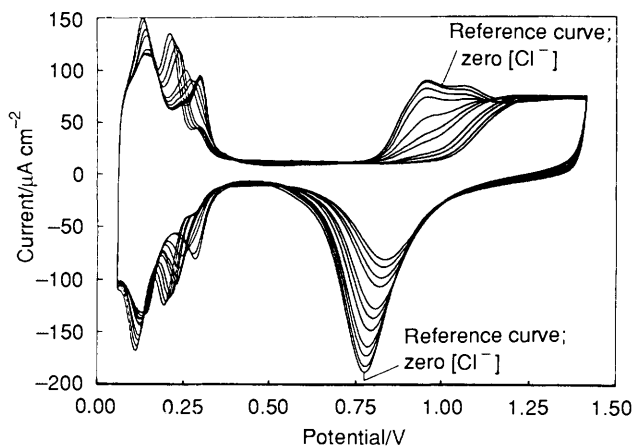


Figure 9 Cyclic-voltammograms for formation and reduction of Pt surface oxide in the presence of progressively increasing Cl^- ion concentration from 10^{-6} to $3 \times 10^{-3} \text{ mol dm}^{-3}$. (From reference 29.)

tally to determine ΔV_e° values (per cm^2) volumetrically in electrode/solution interphases.

7 Competitive Adsorption of Anions in Sub-Monolayer Surface Oxidation Processes

One of the most striking manifestations of specificity of ion adsorption effects is the competitive chemisorption of anions in the early stages of anodic surface oxidation of noble metals.^{28,29} At Pt, the progressive course of sub-monolayer, through monolayer to eventual multilayer surface oxide formation, can be sensitively examined by means of cyclic-voltammetry, a technique in which the current response to a potential signal applied to the electrode is recorded, with the potential being linearly varied in time in a repetitive manner. By micrometric titration of halide ions, X^- , as HX , into dilute aq. HClO_4 , commencing at a concentration of X^- of $10^{-7} \sim 10^{-6} \text{ mol dm}^{-3}$, the progressive adsorption of X^- at a Pt electrode can be accurately followed²⁹ on account of the gradual diminution of surface oxide formation charge and corresponding reduction charge over the potential regions for surface oxide formation and reduction at Pt. The charge for reduction of an OH monolayer at Pt is *ca.* $220 \mu\text{C cm}^{-2}$, a quantity that can be easily and accurately measured in cyclic voltammetry experiments.

The behaviour for Cl^- adsorption²⁹ is shown in Figure 9 which shows that Cl^- initially selectively blocks the surface oxidation up to a potential of +1.1 V vs. RHE. This potential, and the charge involved, corresponds, in the absence of Cl^- , to that for completion, by electrochemical discharge from H_2O , of a monolayer of OH on Pt. Beyond 1.1 V, Cl^- has little further effect. Already at low concentrations, *ca.* $3 \times 10^{-6} \text{ mol dm}^{-3}$, Cl^- adsorption competes with the initial stages of 2-D OH lattice formation on the surface of Pt, represented by processes such as $x\text{-Pt} + \text{H}_2\text{O} \rightarrow \text{Pt}_x\text{OH} + \text{H}^+ + e$, where x represents the number of Pt sites per OH electroadsorbed.

The competitive adsorption isotherm (Figure 10), derived from the results of Figure 9, for the blocking effects of Cl^- on the OH film formation at Pt is a remarkably linear logarithmic relation. Contrarily, for Br^- and I^- adsorption (Figure 10), the competitive adsorption is less selective with regard to blocking up to the OH monolayer limit and follows much more a Langmuir-type of isotherm (sigmoidal dependence of blocking effect on $\log C_{\text{X}^-}$). These results suggest that Cl^- is chemisorbed with only partial transfer of charge ($\text{Cl}^- + \text{Pt} \rightarrow \text{PtCl}^{(1-\delta)} + \delta e$) so that in the adsorbed state it suffers from strong lateral interaction with other $\text{Cl}^{(1-\delta)-}$ species and with discharged OH, giving rise to the logarithmic isotherm of Figure 10, characteristic of long-range repulsive interaction effects in a monolayer. Br^- and I^- seem, on the other hand, to be chemisorbed with

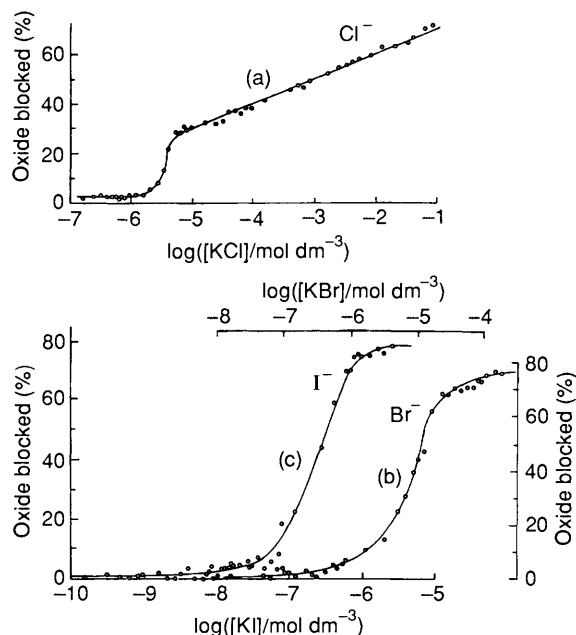


Figure 10 Competitive adsorption isotherms for (a) Cl^- , (b) Br^- , and (c) I^- at Pt from the extents of blocking of surface oxide formation, measured on the reduction sweep as changes of oxide-film reduction charge, Δq . (Data derived from curves such as in Figure 9; from reference 29.)

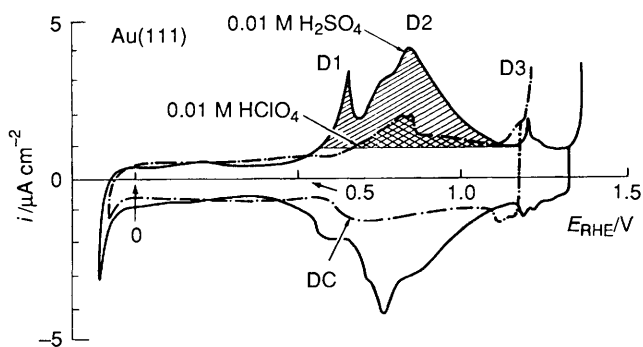


Figure 11 Cyclic-voltammograms for HSO_4^- and ClO_4^- chemisorption with charge transfer at a gold electrode, up to the potential beyond which 2-D surface oxidation of Au just commences (*cf.* reference 28).

almost complete charge transfer so that they reside on the Pt surface as almost neutral atoms, hence with much less repulsion.

At Au, the chemisorption of anions is substantially different: HSO_4^- and ClO_4^- are found²⁸ to be already chemisorbed *prior* to onset of the initial sub-monolayer lattice stages of surface oxide formation and, in fact, cyclic voltammetry on single-crystal Au surfaces²⁸ reveals a kind of reversible underpotential deposition (*cf.* reference 13) current vs. potential profile as illustrated in Figure 11. Thus, the onset of surface oxidation of Au by OH from water takes place *amongst* an initially electroadsorbed lattice of chemisorbed anions.

At Au electrodes, as at Pt at low temperatures,³⁰ the first 5% of a monolayer of OH is reversibly deposited and reduced because it is in a 2-D state on the electrode surface. The formation of this sub-monolayer lattice array is very sensitive to competition by strongly chemisorbed anions, *e.g.* HSO_4^- , as is Pt by Cl^- (Figure 9). Figure 12 shows cyclic-voltammograms for Au surface oxide formation and reduction in dilute aq. HClO_4 over a series of cyclic sweeps to various increasing positive potentials, 'with' and 'without' HSO_4^- anions appreciably adsorbed on the surface. The situation 'without' HSO_4^- is achieved by initially holding the potential in the sweep far

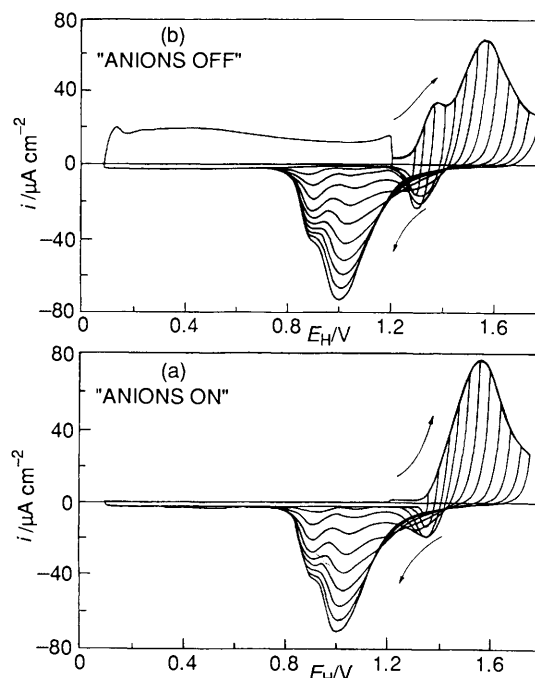


Figure 12 Series of cyclic-voltammograms for surface oxide formation and reduction at gold, taken to successively increasing positive potentials under conditions (a) with adsorbed HSO_4^- anions present on the surface and (b) after their desorption and only incomplete re-adsorption, revealing region of *reversible*, sub-monolayer oxide formation/reduction.

negative to the p.z.c. (so that anions remain unadsorbed) and then returning it at 500 V s^{-1} to the potential for onset of surface oxidation, followed by triggering a normal cyclic sweep at 50 V s^{-1} . When HSO_4^- is present on the surface ('anions on' condition, Figure 12b), the initial *reversible* region of surface oxide formation and reduction at Au, seen when HSO_4^- is 'off' the surface (Figure 12a), is virtually eliminated (Figure 12b).

The processes of development of sub-monolayer levels of electroadsorbed oxygen species at Au, coupled with desorption of previously adsorbed HSO_4^- ions (Figure 11) can be followed successively down to $200 \mu\text{s}$ in time of film growth and to 0.5% in surface coverage by OH or O species, as illustrated in Figure 13.

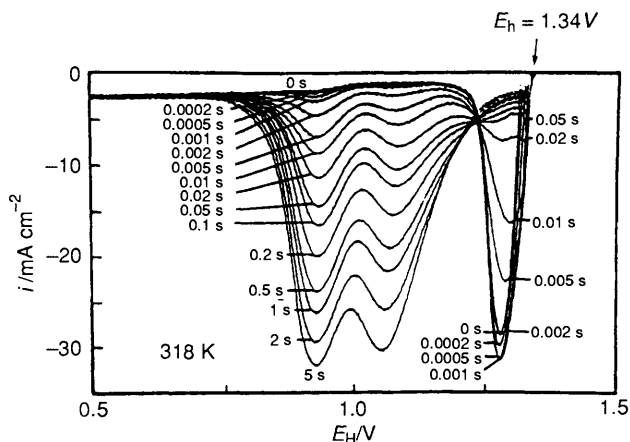


Figure 13 Series of reduction linear sweeps, following successive sub-monolayer surface oxide formation at Au for various times, down to $200 \mu\text{s}$. The series of curves show the progressive interchange of states of the oxide film (as observed in reduction) with time due to (a) anion desorption and (b) coupled OH/Au place exchange. The times indicated are for holding (h) the potential at $E_h = 1.34 \text{ V}$ to allow development of the oxide film, following which cathodic reduction sweeps are initiated to characterize the state and charge for reduction of the anodically formed oxide film.

Here are shown cathodic voltammograms for reduction of sub-monolayer oxide films at Au grown by holding the potential at value $E_h = 1.34$ V (RHE) for controlled times. It is seen that very sensitive measurements of these anion-influenced surface processes can be made, *in situ*, by this electrochemical technique.

8 References

- 1 R. J. Watts-Tobin and N. F. Mott, *Electrochim. Acta*, 1961, **4**, 79.
- 2 S. Trasatti, *J. Chem. Soc., Faraday Trans. 1*, 1972, **68**, 229; *J. Electroanal. Chem.*, 1972, **39**, 163.
- 3 B. E. Conway, *Prog. Surf. Sci.*, 1984, **16** (1), 1.
- 4 J. O'M. Bockris and A. K. Reddy, 'Modern Electrochemistry', Plenum, New York, 1974.
- 5 R. Parsons, 'Modern Aspects of Electrochemistry', Vol. 1, Butterworth, London, 1954, Chapter 3.; see also D. C. Grahame, *Chem. Rev.*, 1947, **41**, 441; and O. Stern, *Z. Elektrochem.*, 1924, **30**, 508.
- 6 B. E. Conway, 'Ionic Hydration in Chemistry and Biophysics', Elsevier, Amsterdam, 1981.
- 7 V. Gutmann, *Chem. Brit.*, 1971, **7** (3), 102.
- 8 G. Nemethy and H. A. Scheraga, *J. Phys. Chem.*, 1962, **66**, 1773; see also A. Ben Naim, 'Hydrophobic Interaction', Plenum, New York, 1980.
- 9 W. Lorenz and G. Salić, *Z. Phys. Chem.*, 1961, N.F. **29**, 390; 408.
- 10 J. W. Schultze and F. D. Koppitz, *Electrochim. Acta*, 1976, **21**, 327; 337.
- 11 D. J. Barclay, *J. Electroanal. Chem.*, 1968, **19**, 318; 1970, **28**, 443.
- 12 W.-K. Paik and J. O'M. Bockris, *Surf. Sci.*, 1971, **27**, 191.
- 13 K. Engelsman, W. J. Lorenz, and E. Schmidt, *J. Electroanal. Chem.*, 1980, **114**, 1.
- 14 T. N. Anderson and J. O'M. Bockris, *Electrochim. Acta*, 1964, **9**, 347.
- 15 W. Schmickler and A. Kornyshev, *J. Electroanal. Chem.*, 1985, **185**, 283.
- 16 D. D. Eley and M. G. Evans, *Trans. Faraday Soc.*, 1938, **34**, 1093.
- 17 K. Heinzinger and P. C. Vogel, *Z. Naturforsch.*, 1976, **31a**, 463; 476; 1974, **29a**, 1169; 1975, **30a**, 789.
- 18 R. N. Butler and M. C. R. Symons, *Trans. Faraday Soc.*, 1965, **61**, 2559.
- 19 B. E. Conway, *J. Solution Chem.*, 1978, **7**, 721.
- 20 B. E. Conway and J. C. Currie, *J. Electrochem. Soc.*, 1978, **125**, 257.
- 21 B. E. Conway, J. E. Desnoyers, and R. E. Verrall, *Trans. Faraday Soc.*, 1966, **62**, 2738.
- 22 R. Zana and E. Yeager, *J. Phys. Chem.*, 1966, **70**, 954; 1967, **71**, 521.
- 23 N. J. Jarvis and M. A. Schieman, *J. Phys. Chem.*, 1968, **72**, 74.
- 24 G. M. Bell and P. D. Rangecroft, *Trans. Faraday Soc.*, 1971, **67**, 649.
- 25 C. Wagner, *Phys. Z.*, 1924, **25**, 474; see also L. Onsager and N. N. T. Samaras, *J. Chem. Phys.*, 1934, **2**, 528.
- 26 B. E. Conway, *J. Electroanal. Chem.*, 1975, **65**, 691.
- 27 H. S. Frank, *J. Chem. Phys.*, 1955, **23**, 2033.
- 28 H. A. Kozłowska, A. Hamelin, and B. E. Conway, *Electrochim. Acta*, 1986, **31**, 1051.
- 29 B. E. Conway and D. M. Novak, *J. Chem. Soc., Faraday Trans. 1*, 1981, **77**, 2341.
- 30 H. A. Kozłowska, B. E. Conway, and W. B. A. Sharp, *J. Electroanal. Chem.*, 1973, **43**, 9.